Current Eye Research, 34, 568–579, 2009

ISSN: 0271-3683 print / 1460-2202 online
DOI: 10.1080/02713680902964892

informa
healthcare

Structural Changes of the Retina after Conventional Laser Photocoagulation and Selective Retina Treatment (SRT) in Spectral Domain OCT

Carsten Framme, Andreas Walter, Philipp Prahs, and Roman Regler
University Eye Hospital, Regensburg, Germany

Clemens Alt
Wellman Center for Photomedicine, Massachusetts General Hospital, Harvard Medical School, Boston, Massachusetts, USA

Dirk Theisen-Kunde
Medical Laser Center, Luebeck, Germany

Ralf Brinkmann
Medical Laser Center, Luebeck, Germany

ABSTRACT

Background: Spectral domain optical coherence tomography (SD-OCT) in patients can deliver retinal cross-sectional images with high resolution. This may allow the evaluation of the extent of damage to the retinal pigment epithelium (RPE) and the neurosensory retina after laser treatment. This article aims to investigate the value of SD-OCT in comparing laser lesions produced by conventional laser photocoagulation and selective retina treatment (SRT). *Material and Methods:* In a retrospective study, conventional retinal laser (CRL) lesions and SRT laser lesions were evaluated with SD-OCT. One hundred seventy-five CRL lesions were investigated in 10 patients with diabetic maculopathy at timepoints between 1 hr and 4 years after treatment. Ninety-one SRT lesions were examined in 9 patients with central serous retinopathy, geographic atrophy, and diabetic maculopathy at timepoints between 1 hr and 2 years. CRL lesions were applied with an ophthalmoscopically slightly grayish-white appearance (Nd:YAG laser at 532-nm wavelength; power 100–200 mW; retinal spot diameter 100 μm; pulse duration 100 ms). SRT lesions were applied with a Nd:YLF (527 nm; pulse duration 200 ns [30 pulses at 100 Hz]; energy 100–200 μJ/pulse; retinal spot diameter 200 μm) and were visible only angiographically. *Results:* All CRL lesions were characterized by high reflectivity in OCT images throughout the full thickness of the neurosensory tissue 1 hr after irradiation, suggesting complete neurosensory coagulation. Strong contraction through the full thickness of the neurosensory layers was observed within 7 days after treatment. In contrast, the neural retina appeared unaffected after SRT. For both lesion types, the RPE layer appeared to be regular or thinner immediately after treatment, whereas within a period of 4 weeks, a RPE thickening indicating RPE proliferation was observable. One year and later after treatment, CRL lesions were characterized by RPE atrophy combined with significant damage of the neurosensory tissue. SRT lesions aged one year and older revealed unaffected neurosensory structures and an intact RPE layer. *Conclusion:* Spectral domain OCT can be used clinically to follow the development of laser-induced lesions over time. Postoperative RPE proliferation was observed in both CRL and SRT laser lesions. RPE atrophy

Received 22 September 2008; Accepted 12 April 2009.

Correspondence to: Carsten Framme, FEBO, MHM®, MBA, University Eye Hospital Regensburg, Franz-Josef-Strauss-Allee 11, D-93042, Regensburg, Germany. E-mail: carsten.framme@klinik.uni-regensburg.de

appeared subsequently only in CRL lesions, whereas the neurosensory retina appeared unaffected following SRT. These results suggest the selective effect of SRT in humans without causing adverse effects to the neurosensory retina.

Keywords: autofluorescence; imaging; OCT; retinal laser treatment; SRT

INTRODUCTION

Conventional laser photocoagulation has been shown to successfully manage complications in a variety of retinal diseases such as diabetic macular edema (DME), diabetic retinopathy (DRP), macular edema in branch retinal vein occlusion (BRVO), or central serous chorioretinopathy (CSC). There is substantial evidence that the positive laser effect is mediated by the retinal pigment epithelium (RPE).[1,2] The RPE, due to its high amount of melanosomes, absorbs about 50 to 60% of incident green light, and, thus, it is the main target of laser energy applied to the retina.[3] During typical coagulation, exposure times of about 100–200 ms thermal heat conduction from the center of the laser burn toward the periphery, and into the neurosensory retina results in the formation of an ophthalmoscopically visible grayish-white lesion. Histologically, primary damage of the RPE was observed, with associated coagulative tissue changes in the outer and inner segments of the photoreceptors.[4–7] Several groups studied effects of laser treatment on the fundus. *In vivo* it was shown that argon laser photocoagulation of the monkey and human fundus causes necrosis of the RPE and a detachment of the RPE from Bruch's membrane,[8–10] budding of individual RPE cells,[10,11] and a multilayered RPE formation in the area of laser irradiation by 7 days after treatment.[1,8–10,12,13] Histology immediately after conventional argon laser treatment showed that all RPE cells are destroyed, and the choriocapillaris as well as the vessels of the choroid are damaged.[14] RPE cells adjacent to the laser lesion appear to migrate into the lesion and proliferate, covering the tissue defect.[15] The RPE barrier was completely restored 7 days after mild macular coagulation.[15] Thus, proliferation of RPE cells can be interpreted as the primary healing response to defects in the RPE monolayer.

Several macular diseases, e.g., age-related macular degeneration, CSC, or DME, are also thought to be caused by reduced functionality of the RPE cells.[16–18] Therefore, a method for the selective "stimulation" of RPE cells without causing adverse effects to choroid and neuroretina, especially to the photoreceptors, might be an appropriate treatment assuming that the barrier is restored quickly after treatment.[19] The selective effect on RPE cells has been demonstrated initially by using 5-μs argon laser pulses at 514 nm with a repetition rate of 500 Hz.[19] By irradiating the fundus with a train of microsecond laser pulses, it is possible to achieve high peak temperatures around the melanosomes, leading to damage of the RPE.[9] Due to the short pulse duration, heat diffusion is minimized and sublethal temperature increase is observed in adjacent tissue structures.[9] The selective damage of the RPE cells with concurrent sparing of photoreceptors has been confirmed by histology at different times after treatment.[20,21] The first clinical trial of selective retina treatment (SRT) using a Nd:YLF laser system with a pulse duration of 1,7 μs (100 pulses, 100 and 500 Hz) demonstrated the clinical potential of this technique.[22,23] Subsequently, SRT laser parameters were successfully refined, reducing the applied energy by using even shorter pulses, fewer repetitive pulses, and lower repetition rates.[24] Additionally, efforts were undertaken to non-invasively visualize the ophthalmoscopically invisible SRT lesions postoperatively by fundus autofluorescence (AF), which was also able to show proliferation effects of the RPE days to weeks after the SRT and also the conventional laser treatment.[25,26]

Since the SRT effect has only been histologically proven in rabbit trials so far, the advent of spectral domain optical coherence tomography technique (SD-OCT) might be able to achieve this goal non-invasively also in human treatments. The SD-OCT provides cross-sectional retinal images with an axial resolution of about 7 μm. Thus, axial resolution is on the order of the thickness of the RPE monolayer, and structural changes within the retina might now be detected with sufficient sensitivity. The aim of this study was to investigate the value of SD-OCT for the post-treatment control after SRT by comparing retinal tissue changes in conventional retinal laser (CRL) lesions and SRT lesions in patients.

MATERIAL AND METHODS

SD-OCT

Fundus and OCT images were acquired with a combined SD-OCT and scanning laser ophthalmoscope (SLO) imaging system (Spectralis HRA+OCT; Heidelberg Engineering, Heidelberg, Germany). The system is able to acquire en face SLO images in angiographic, AF, and reflectance imaging modes as well as cross-sectional SD-OCT images. An 870-nm super luminescent diode (SLD) is used for OCT imaging. In SD-OCT

mode, the retina is scanned at 40.000 A-scans per second, presenting highly detailed images of the retinal structure. The OCT depth resolution (FWHM) is 7 μm. The images of the SLO and OCT modes can be overlaid and automatically, spatially co-registered. Images can also be co-registered over time for different visits of a patient.

Patients and Qualitative Grading of Laser Lesions

Images were recorded to evaluate the appearance of the retinal laser lesions in patients with DME, CSC, and geographic atrophy (GA) due to age-related macular degeneration (AMD).

OCT imaging after laser treatment was performed on a total of 266 lesions in 19 patients presenting both CRL and SRT lesions. One hundred seventy-five CRL lesions were investigated in 10 patients with DME at timepoints between 1 hr and 4 years after treatment. Ninety-one SRT lesions were examined in 9 patients with CSC, GA, and DME at timepoints between 1 hr and 2 years. Each patient underwent complete ophthalmologic examination. In most cases, additional angiography and AF was performed. OCT evaluation focused on analyzing the appearance of both the RPE and the neurosensory retinal layers within the lesion sites. Herein, the RPE was qualitatively graded as (1) regular, (2) thin, (3) thick, or (4) atrophic. The neurosensory layer was graded as being (1) regular, (2) of increased reflectivity, or (3) of contracted appearance. In selected cases, the OCT findings were compared to the AF levels in the irradiated areas. The exact location of lesions in the images are demarked with arrows deduced from distance measurements in the Eye Explorer software (Heidelberg Engineering, Heidelberg, Germany).

Laser Settings

Conventional laser photocoagulation treatment was carried out using a Nd:YAG laser (Visulas, Zeiss, Jena, Germany; wavelength 532 nm frequency-doubled; retinal spot diameter 100 μm; duration 100 ms, and power 100–200 mW). SRT was carried out using an experimental prototype of an SRT laser system (SRT Laser vario; Medical Laser Center Luebeck, Germany). The laser was manufactured in accordance with the European Medical product law. The core of the system consists of a diode laser excited Q-switched Nd:YLF-laser with intracavity frequency conversion to a wavelength of 527 nm. The duration of the Q-switched pulse can be extended from 200 ns up to 3 μs by increasing the efficiency of the second harmonic generation up into the overcoupling regime.[27] The laser was operated at a repetition rate of 100 Hz, and a train of 30 pulses (each of 200 ns pulse length) was applied to generate the SRT lesions. Maximal pulse energy of this laser system was 1 mJ.

Laser Treatment

Proper SRT dosimetry of the ophthalmoscopically invisible lesions was adjusted in each patient by placing 4 to 16 test exposures with energies ranging from 60–200 μJ at the lower vessel arcade. The energy was increased in increments of 20 μJ up to the level where test exposures became ophthalmoscopically visible or up to the highest energy of the laser. Afterwards, angiography was performed to determine the angiographic visibility that indicates the desired RPE damage. Treatment lesions then have been applied with energies within the therapeutic window between the angiographic and ophthalmoscopic threshold. The SRT treatment was approved by the local ethics committee, and a written consent was obtained from each patient.

The therapeutic results of SRT in these patients will be discussed elsewhere. In certain diseases, such as DME or CSC, previous clinical studies showed improvement in the course of the disease.[23,25] In this study, in a new subgroup of patients presenting with bilateral and equally pronounced GA due to AMD, one eye was treated by SRT in the junctional zone of the atrophy. The rationale is based on AF findings in GA that mostly reveal increased AF signals in the junctional zone of atrophy, suggesting RPE cells with a high lipofuscin content designated for apoptosis.[28] It was the purpose ideally to stop or reduce further growth of atrophy by irradiating the junctional zone, thus to stimulate the cells to proliferate. These clinical results will also be discussed elsewhere.

RESULTS

In this study, significant differences of tissue changes between CRL lesions and SRT lesions were detected using SD-OCT. Ophthalmoscopically, CRL lesions were frequently visible as grayish-white coagulation spots, while all SRT lesions were ophthalmoscopically invisible. The observed retinal structural changes of both lesion types are summarized for all patients in Table 1 (CRL lesions) and Table 2 (SRT lesions).

CRL Lesions

SD-OCT images taken 1 hr after treatment showed increased reflectivity throughout the full thickness of the neurosensory layer within all observed CRL lesions (Fig. 1). Also, retinal structure and delineation of the individual layers comprising the retina were lost, similar to histologic findings after laser photocoagulation. The

Table 1. Characteristics of conventionally applied laser lesions in 10 patients with diabetic maculopathy. Displayed are patients' age, the age of CRL lesions, the number of lesions, and the corresponding figures. A description of the RPE and the neurosensory layer derived from the OCT sections are given using the following terms: RPE is described as being (1) regular, (2) thin, (3) thick, or (4) atrophic; for the neurosensory layers, reflectivity is described as (1) regular, (2) increased, or (3) contracted. Additional information is given for increased (AF+) or decreased (AF–) autofluorescence of the distinct lesions if available

Patient	Age	Age of lesions	Number of lesions	RPE	Fundus-autofluorescence	Neurosensory layers reflectivity	Figures
1	56	1 hr	$n = 12$	Thin		Increased	Figs.1 and 2
		1 wk	$n = 12$	Thick		Contracted	
		1 yr	$n = 20$	Thick		Increased	
2	70	1 hr	$n = 14$	n.d.		Increased	
3	83	3 yr	$n = 17$	Atrophic		Contracted	
4	72	1 hr	$n = 8$	Regular	AF+	Increased	Fig. 3
		8 mo	$n = 23$	Thick		Contracted	
5	71	6 mo	$n = 7$	Thick	AF+	Increased	
		3 yr	$n = 11$	Atrophic	AF–	Contracted	
6	65	1 yr	$n = 19$	Thick	AF+	Increased	
		4 yr	$n = 13$	Atrophic	AF–	Increased	
7	71	3 wk	$n = 26$	Thick		Contracted	Fig. 4
8	60	14 mo	$n = 14$	Thick	AF+	Contracted	Fig. 5
		3 yr	$n = 11$	Atrophic	AF–	Contracted	
9	63	4 wk	$n = 18$	Thick		Increased	
10	64	8 mo	$n = 8$	Thick	AF+	Contracted	
		16 mo	$n = 6$	Atrophic	AF–	Contracted	

(n.d. = non-determinable).

RPE as the primary absorber of laser energy in part appeared thinned 1 hr after treatment due to the significant damage to this layer (Patient 1; Table 1). However, RPE thinning after coagulation was not observed in all lesions, and then the RPE signal was within the regular range (Patient 4; Fig. 3; Table 1). The CRL lesions in Patient 1 showed, upon reexamination after one week, thickening of the RPE within the lesion sites (Fig. 2). In addition, contraction of the neurosensory layers appeared in all lesions, suggesting scarring of the tissue (Figs. 1 and 4). The extent of contraction was different in patients; however, increased reflectivity at the lesion sites was always apparent in one-week up to 4-year-old lesions. In general, the grade of this reflectivity increase was more enhanced 1 hr after laser photocoagulation than in older lesions, when tissue contraction was predominantly visible.

CRL lesions 3 years and older revealed complete RPE atrophy and an increased OCT signal within the choroidal layer. Younger lesions between 1 and 3 years in age were characterized by RPE thickening in the center of the lesion surrounded by atrophic RPE (Fig. 5A2), further leading to complete atrophy. This is consistent with the AF appearance of those lesions showing a central island of increased AF surrounded by an atrophic ring without any AF signal (Fig. 5C). As displayed in Fig. 5B2, final complete RPE atrophy in accordance to the negative AF (Fig. 5C) was observed.

SRT Lesions

In contrast to the CRL lesions, regular RPE and regular neurosensory structures were observed in 5 patients (33 lesions) 1 hour after SRT (Figs. 6, 7, and 8; Table 2). Although significant postoperative angiographic leakage demonstrated clear RPE damage, no alterations of the RPE signal were visible in SD-OCT. Additionally, no alterations of the neurosensory tissue were observed in any of these early lesions. This absence of neuroretinal changes in the OCT images confirms the selective effect of SRT. Follow-up of the SRT lesions up to 5 months also confirmed expected thickening of the RPE layer in all lesions, which agrees well with the increase of AF intensity within the lesion sites 3 weeks after irradiation (Fig. 8D). Despite these changes in the RPE layer over the course of the recovery, the neurosensory layer remained regular at any timepoint during follow-up. However, in solitary lesions, some affection of the outer photoreceptor layers might not be completely ruled out (Fig. 7A; Fig. 8E). Herein, RPE proliferation in the center of such lesions seemed to push the

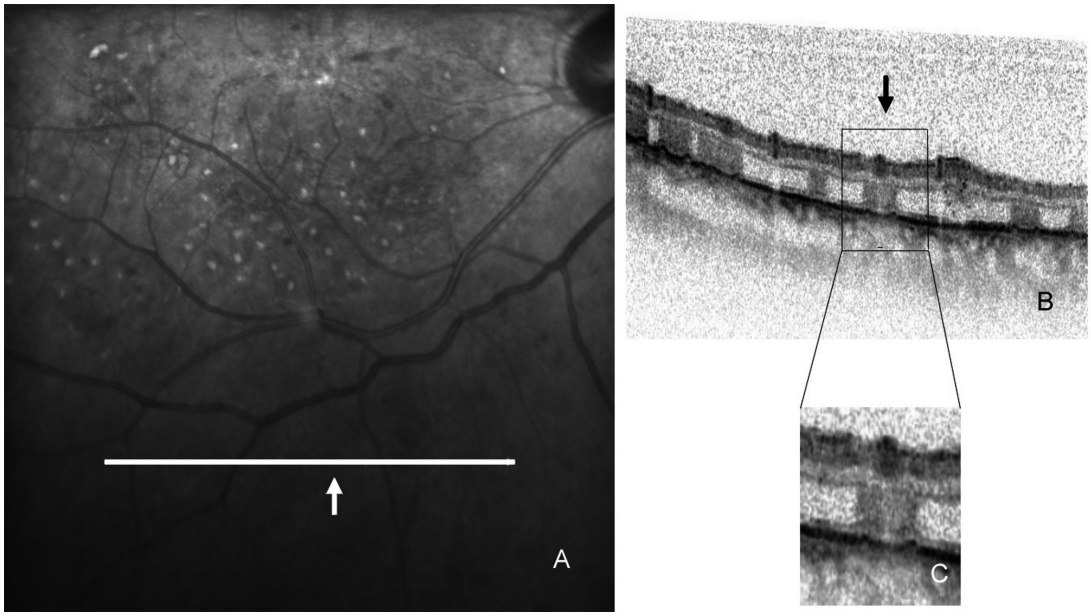

Figure 1. OCT image on CRL lesions 1 hr after treatment. (A) IR fundus image shows slightly visible neurosensory retinal coagulation at the lower vessel arcade. (B) OCT image shows significantly increased reflectivity and loss of structure throughout the full-thickness retina, while the RPE appeared thinner at the lesion sites. Arrows demarcate one of the laser lesions, magnified in (C).

outer and inner layer of photoreceptors inwards (Figs. 7 and 8); however, OCT images did not allow for further differentiation of this possible damage to the outer photoreceptor layer.

The described features of selective RPE changes were observed in SRT lesions up to 20 months of duration after treatment, with no hints of atrophic RPE appearance (Fig. 9).

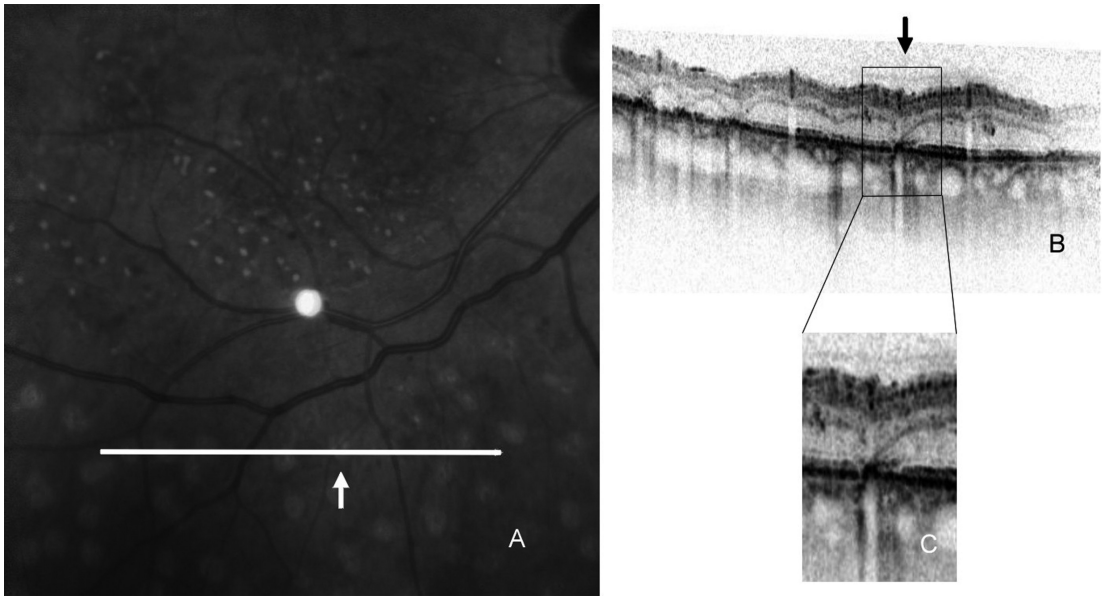

Figure 2. Same OCT section from Figure 1 one week after treatment. (A) IR fundus image shows increased visibility of the laser burns. (B) OCT image shows significant full-thickness alterations of the neurosensory retina in all of the lesions, such as contraction and an arcade-like appearance of the inner layers. The RPE within the lesion sites appeared to be thicker, suggesting RPE proliferation. Arrows demarcate the same lesion (also magnified in C) as displayed in Figure 1.

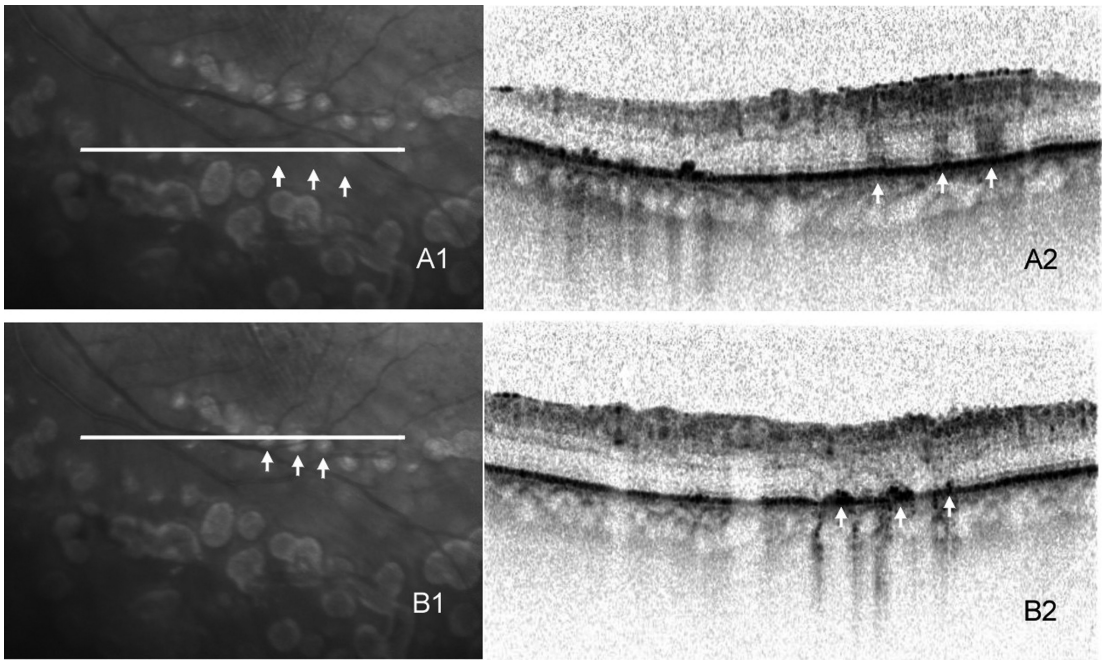

Figure 3. CRL lesions aging 1 hr (A) and 8 months (B) are displayed (arrows demarcate particular lesions). In section A, three lesions are displayed with increased reflectivity of the neurosensory layers but—in contrast to Figure 1—regular RPE. In section B, RPE thickening suggesting the proliferation process was observed. Also, the choroidal signal was decreased within these lesions, while it was enhanced at the rim and in between the lesions, suggesting RPE atrophy. Additionally significant alterations of the neurosensory layers (increased reflectivity indicating coagulation as well as tissue contraction) were seen.

DISCUSSION

High-resolution SD-OCT allows clinical evaluation of the extent of retinal laser damage after conventional laser photocoagulation and SRT. Especially, the combination of OCT with the different confocal SLO imaging modalities, as well as the image registration and tracking, allows following particular laser lesions from the time of treatment over the period of the recovery process.

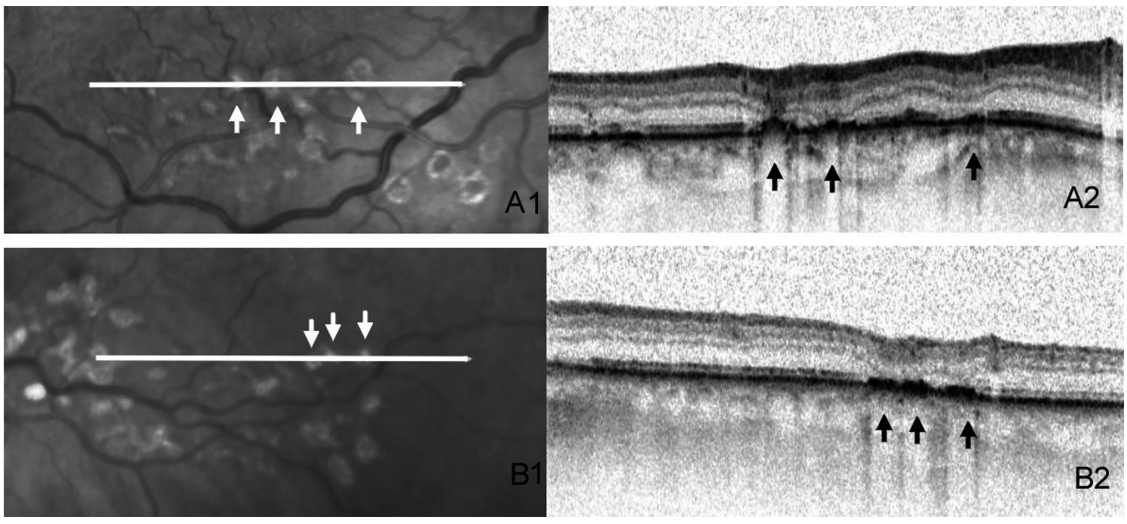

Figure 4. Two OCT sections (A2, B2) with their corresponding fundus IR images (A1, B1) in 3-week-old CRL lesions in both eyes of a 71-year-old patient. Arrows demarcate three particular lesions in each of the sections. RPE thickening and full-thickness high reflectivity and contraction of the neurosensory tissue (A2, B2) suggest thermal coagulation. Pushed-up RPE in the left lesion (A2) might also indicate choroidal coagulation.

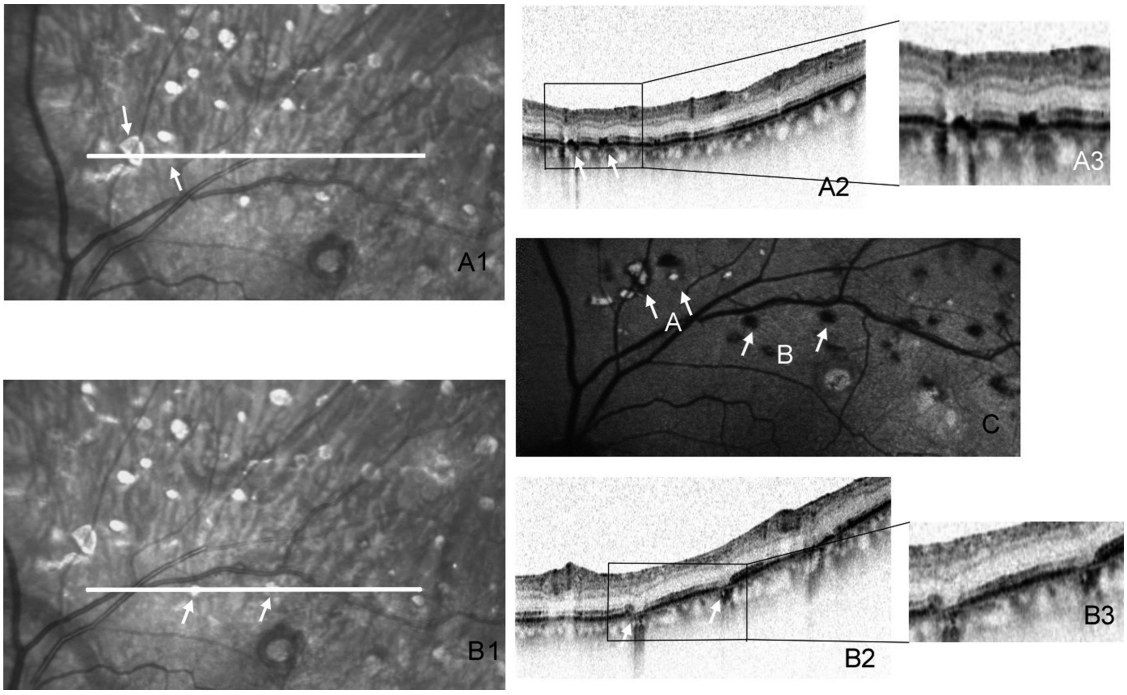

Figure 5. Displayed are two OCT sections and their corresponding IR images (A, B) and an AF image (C) of the left fundus from a 60-year-old patient presenting CRL lesions (arrows). The A images (labeled A in C) showed 14 months of CRL lesions of increased AF. The CRL lesions of the B images (labeled B in C) were three years old, presenting no AF signal (C). The AF-positive CRL lesions were characterized by thickened RPE and contraction of the neurosensory layer (A2, magnified in A3), indicating RPE proliferation. The AF-negative lesions (B2, magnified in B3) revealed RPE atrophy and enhanced reflectivity of the choroid.

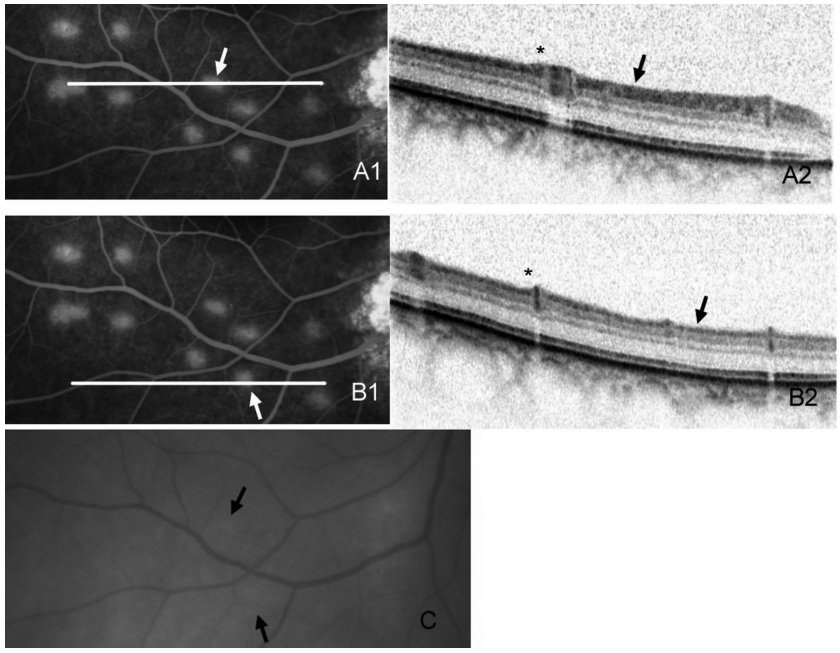

Figure 6. SRT lesions aged 1 hr are displayed angiographically in two sections, revealing progressive leakage from the selectively damaged RPE (A1, B1 = angiography; arrows demarcate distinct lesions). OCT sections (A2, B2) showed normal reflectivity of the neurosensory retinal layers underlining the selective effect of SRT (arrows demarcate the location of the distinct lesions; * = retinal blood vessels). The lesions were ophthalmoscopically invisible (C), suggesting unaffected neurosensory tissue.

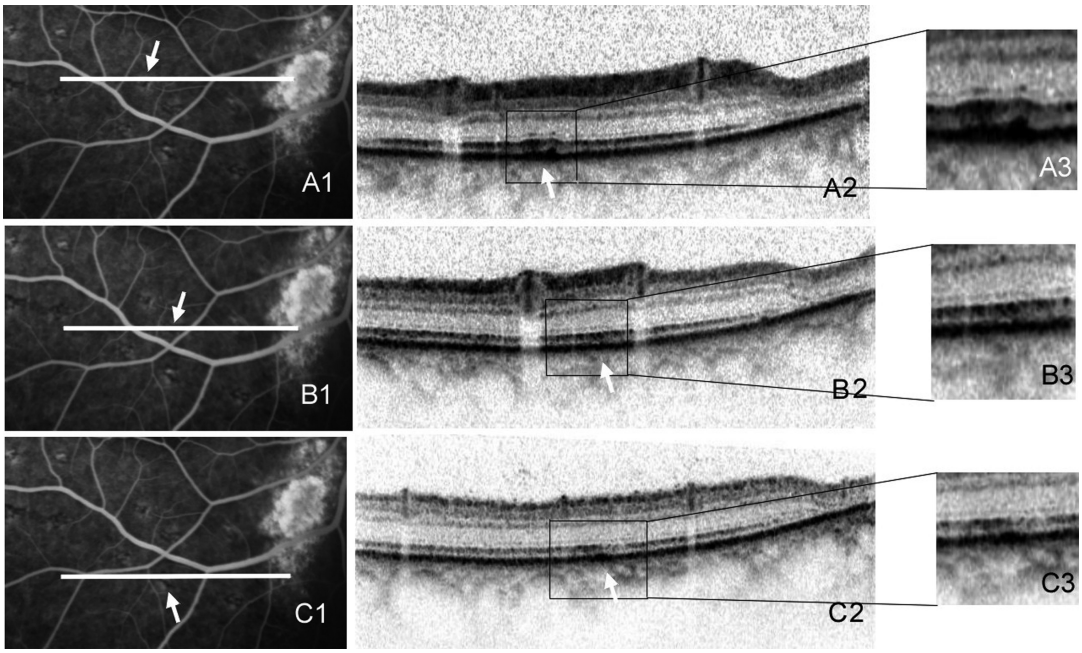

Figure 7. The same lesions from Figure 6 are displayed two weeks later in three sections (A1, B1, C1). The OCT showed a variable thickening of the RPE layer, suggesting RPE proliferation (A2 and C2, magnified in A3 and C3). Neurosensory retinal layers, including the outer photoreceptor layers appeared mostly unaffected in all SRT lesions; however, some slight structural changes might be observed within the outer photoreceptor layer in particular lesions (A3).

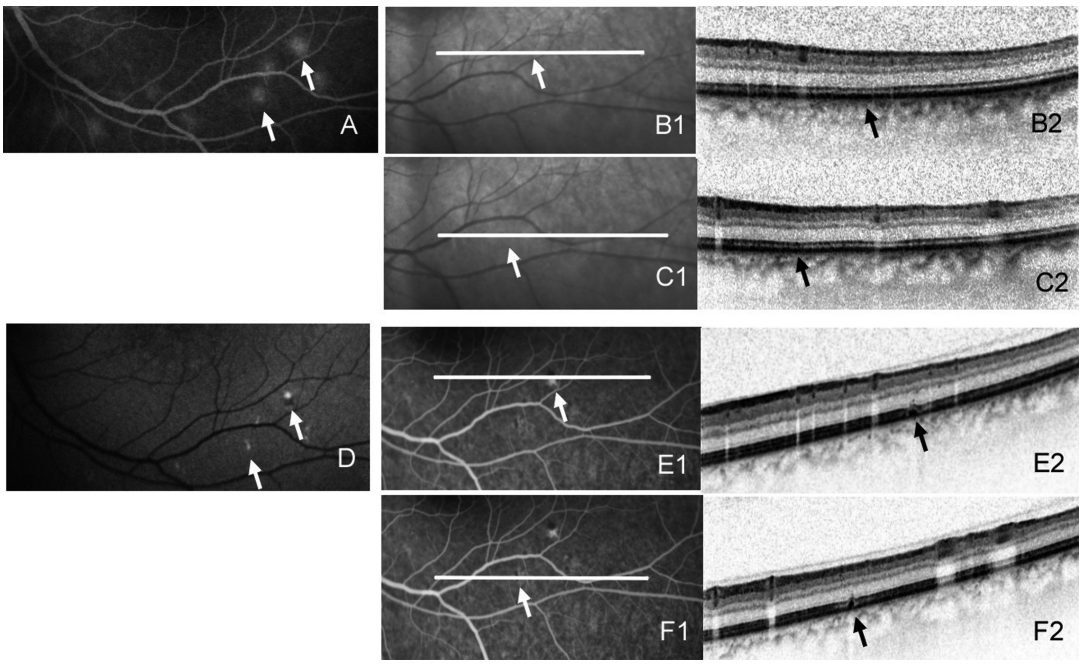

Figure 8. Displayed are SRT lesions 1 hr after treatment (A = FLA; arrows demarcate distinct lesions) with corresponding IR image (B1, C1) and the OCT sections (B2 and C2). The same lesions 3 weeks later are shown in AF image D (arrows again demarcate same lesions) with the corresponding OCT sections (E1–2 and F1–2]. One hour after treatment for fluorescein-positive SRT lesions (A), no structural changes were seen in OCT (B2, C2). Three weeks later, lesions revealed increased AF levels (D), indicating RPE proliferation, while OCT sections presented marked RPE thickening in the center of the lesions without damage to the neurosensory layers (arrows) (E2, F2). This underlines the considered selective RPE proliferation, whereas the decreased reflectivity at the lesions periphery might be derived from some still apparent leakage inducing small edema within the outer photoreceptor layers. The inner retinal layers are unaffected and only "pushed" a little inward due to the RPE thickening (F2, arrow).

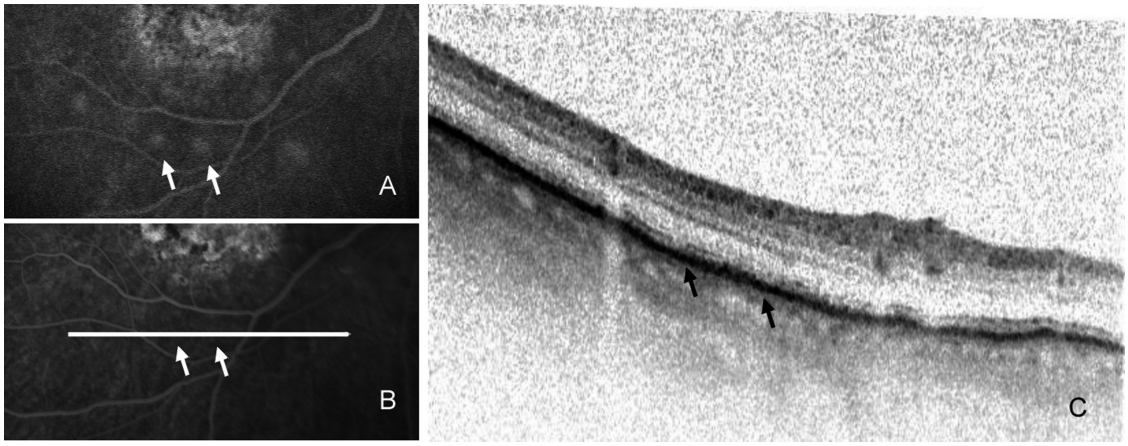

Figure 9. 14-month-old AF- and FLA-positive SRT lesions (A, B; arrows demarcate distinct lesions) showed regular RPE (C; arrows demarcate the location of the lesions) with no signs of atrophy or irregular neurosensory retina. No laser-induced RPE atrophy is expected due to the absence of damage to the neurosensory and choroidal layers.

Table 2. Characteristics of SRT laser lesions in nine patients with different macular diseases (CSC = central serous chorioretinopathy; GA = geographic atrophy due to AMD; DME = diabetic macular edema). Displayed are patients disease, patients' age, age of SRT lesions, number of lesions, and corresponding figures. A description of the RPE and the neurosensory layer derived from the OCT sections is given using the following terms: RPE is described as being (1) regular, (2) thin, (3) thick, or (4) atrophic; for the neurosensory layers reflectivity is described as (1) regular, (2) increased, or (3) contracted. In one case, neurosensory irregularities were observed due to a neurosensory detachment. Additional information is given for increased (AF+) or decreased (AF–) autofluorescence of the distinct lesions if available

Patient	Age	Age of lesions	Number of lesions	RPE	Fundus-autofluorescence	Neurosensory layers	Figures
1 CSC	49	1 hr	$n = 8$	Regular		Regular	
2 CSC	58	1 hr	$n = 7$	Regular		Regular	Figs. 6 and 7
		2 wk	$n = 7$	Thick		Regular	
3 CSC	51	1 hr	$n = 5$	Regular	AF+	Regular	
		4 wk	$n = 5$	Thick		Regular	
4 CSC	39	1 hr	$n = 6$	Regular	AF+	Regular	Fig. 8
		3 wk	$n = 6$	Thick		Regular	
5 CSC	49	1 hr	$n = 6$	Regular		*Irregularities due to neurosensory detachment*	
		2 wk	$n = 6$	Thick			
		3 mo	$n = 6$	Thick			
6 CSC	45	1 hr	$n = 7$	Regular		Regular	
		2 mo	$n = 7$	Thick		Regular	
		5 mo	$n = 7$	Thick		regular	
7 GA	81	14 mo	$n = 4$	Thick	AF+	Regular	Fig. 9
8 GA	67	19 mo	$n = 2$	Thick	AF+	Regular	
9 DME	68	20 mo	$n = 2$	Thick		Regular	

(n.d. = non-determinable).

In general, the tissue response in RPE and neural retina involved in the recovery processes after laser impact for conventional and SRT laser treatment can be followed in detail. The OCT findings in turn correlate well with AF findings, demonstrating that the well-known histological features can be monitored in a non-invasive manner *in vivo* also in humans.

CRL Lesions

Early CRL lesions 1 hr after treatment frequently revealed a thinner or regular RPE layer in OCT imaging corresponding to histological findings showing damaged RPE cells.[1,7,14,15] Since the debris of damaged RPE cells are expected to still be in place immediately after treatment, variances of the OCT signal from the RPE layer are obvious (regular versus thin appearance regarding to Table 1). In no case was a thickening of the RPE observed 1 hr after treatment; however, always a full-thickness increase of reflectivity within the neurosensory retina was seen, indicating complete thermal coagulation that accounts for the ophthalmoscopic visibility of these lesions. Thus, SD-OCT is able to non-invasively demark morphologically a full-thickness damage of the retina, which might also account for a reduced AF signal usually seen in these lesions[26] by simply blocking the RPE-derived AF.

Within days after laser treatment, the cell debris of damaged RPE cells and photoreceptors is phagocitized by RPE bystander cells sliding in from the neighborhood or by macrophages originating from the choriocapillaris.[1,8–10,12,13,29] Such lesion sites show significantly increased AF in this phase of the recovery.[25,26] Accordingly, in our study, RPE thickening in CRL lesions was frequently found in OCT 1 week and later after treatment, suggesting the described RPE proliferation. A decreased OCT signal within the choroid always accompanied these RPE changes due to stronger bulk absorption in the thicker and presumably multilayered RPE layer. Regarding the neurosensory tissue in all lesions, significant full-thickness damage could be followed, showing high reflectivity accompanied by loss of tissue structure and subsequent tissue contraction, which suggests an irreversible impact of the cw laser photocoagulation.

Finally, RPE atrophy was always present in CRL lesions several years of age. Usually, spots without any AF signal indicate complete loss of RPE for such lesions, as also observed in GA due to AMD.[28] Accordingly, the OCT images revealed atrophic RPE layers and enhanced OCT intensity in the choroidal layers due to the lost RPE absorption. This underlines the irreversible process of cw laser-induced scotoma and suggests that a lack of proper support function by, for example, healthy photoreceptor structures prevents a recovery of a stable and healthy RPE layer after conventional laser photocoagulation.

SRT Lesions

Early SRT lesions 1 hr after treatment revealed regular RPE signals and, in contrast to the CRL lesions, no structural changes of the neurosensory layer. This suggests that the laser impact is, as expected, selective to the RPE by lacking damage to the photoreceptors and inner neurosensory layers. As derived from Fig. 6 and Fig. 8, angiography clearly demonstrates the SRT-induced RPE damage by revealing leakage, with no signs of damage in the corresponding OCT signal. Thus, using the SD-OCT technique, it is possible for the first time to non-invasively visualize the selective effect of SRT in humans. Regarding retinal function of such laser lesions, microperimetry has already been successfully performed and revealed no laser scotoma resulting from the treatment.[21,22] However, it has been discussed whether the microperimetry stimulus was small enough to prove this sufficiently. Conversely, the presented OCT findings confirm the microperimetric findings by suggesting intact neurosensory structures.

Since early ophthalmoscopically invisible SRT lesions as well as ophthalmoscopically visible CRL lesions reveal an AF decrease of unknown origin,[25,26] this seems to be derived from a lack of proper fluorophores due to the laser-induced RPE damage but not—as suggested by the OCT findings—from a blockage phenomenon or even from sub- or intraretinal fluid, which was not noticed herein in the OCT sections.

SRT lesions are characterized by a similar early RPE recovery phase in that RPE thickening suggests proliferation. Comparable to CRL lesions aging 1 week and older, such SRT lesions also reveal significantly increased AF. As shown in Figure 8, the increased AF levels correlate well with the thick RPE signal in the OCT section underlining the RPE healing mechanism.

This process was independent from different macular diseases or patients' age and can therefore be considered as being autonomous from a potential neurosensory damage. However, it was remarkable to observe the significant absence of structural changes within the neurosensory retinal layer in SRT lesions. In contrast to the full-thickness damage in CRL lesions, no neural retinal alterations, except of slight photoreceptor changes in some lesions, were observed at any timepoint during follow-up in any of the SRT lesions.

Moreover, no atrophy of the RPE layer was found after about 2 years from treatment with SRT underlining

the proposed selective effect. While, however, only a small number of older SRT lesions was examined in this study, the lack of RPE atrophy suggests integrity of the choroid and neurosensory retina. That is, selective RPE targeting spares not only the neural retina but also the oxygen-rich choroid from thermal coagulation. As a result, a fully functional, healthy and stable RPE can regenerate. However, a larger number of older SRT lesions needs to be examined to achieve concluding results on this issue.

SUMMARY

In summary, the recent advent of clinically available high-resolution SD-OCT allows distinct examination of retinal tissue changes after laser treatments for the first time. This study highlights the dramatically different tissue reactions after conventional thermal laser photocoagulation and SRT laser treatment. Even in the small patient series of this pilot study, the selective effect of SRT was contrasted against the irreversible full-thickness damage of photocoagulation in a non-invasive manner *in vivo*. RPE thickening demonstrated the proliferation process after treatment in both laser lesion types; however, final RPE atrophy was only observed for CRL but not for SRT lesions.

Further OCT studies examining a larger number of laser lesions might be able to evaluate the presented tissue changes also quantitatively. Moreover, future generations of OCTs may have an even better resolution and may be able to display the RPE photoreceptor complex in more detail in order to evaluate the laser impact in these layers more exactly.

ACKNOWLEDGMENT

The authors would like to thank the Dr. Werner Jackstaedt foundation in Wuppertal, Germany, for the generous financial support of this ongoing study.

REFERENCES

1. Marshall J, Clover G, Rothery S. Some new findings of retinal irradiation by krypton and argon lasers. In: Birngruber R, Gabel VP, eds. Laser treatment and photocoagulation of the eye. *Doc Ophthalmol Proc Series.* The Hague: Junk Publ, 1984;36:21–37.
2. Tso MOM, Cunha-Vaz JG, Shih C, Jones CW. Clinicopathologic study of blood-retinal barrier in experimental diabetes mellitus. *Arch Ophthalmol.* 1980;98:2032–2040.
3. Gabel VP, Birngruber R, Hillenkamp F. Visible and near infrared light absorption in pigment epithelium and choroid. In: Shimizu K, ed. International Congress Series No. 450, XXIII Concilium Ophthalmologicum, Kyoto. Princeton, NJ: Excerpta Medica; 1978:658–662.
4. Birngruber R. Die Lichtbelastung unbehandelter Netzhautareale bei der Photokoagulation. *Fortschr Ophthalmol.* 1984;81:147–149
5. Lorenz B, Birngruber R, Vogel A. Quantifizierung der Wellenlängenabhängigkeit laserinduzierter Aderhauteffekte. *Fortschr Ophthalmol.* 1989;86:644–654.
6. Marshall J, Mellerio J. Pathological development of retinal laser photocoagulations. *Exp Eye Res.* 1968;7:225–230.
7. Wallow IH, Birngruber R, Gabel VP, Hillenkamp F, Lund OE. Netzhautreaktion nach Intensivlichtbestrahlung. *Adv Ophthalmol.* 1975;31:159–232.
8. Smiddy WE, Fine SL, Quigley HA, et al. Comparison of krypton and argon laser photocoagulation: Results of simulated clinical treatment of primate retina. *Arch Ophthalmol.* 1984;102:1086–1092.
9. Smiddy WE, Fine SL, Quigley HA, et al. Simulated treatment of recurrent choroidal neovascularization in primate retina: Comparative histopathologic findings. *Arch Ophthalmol.* 1985;103:428–433.
10. Smiddy WE, Fine SL, Quigley HA, et al. Cell proliferation after laser photocoagulation in primate retina: An autoradiographic study. *Arch Ophthalmol.* 1986;104:1065–1069.
11. Marshall J, Bird AC. A comparative histopathologic study of argon and krypton laser irradiations of the human retina. *Br J Ophthalmol.* 1979;63:657–668.
12. Matsumoto M, Yoshimura N, Honda Y. Increased production of transforming growth factor-b2 from cultures human retinal pigment epithelial cells by photocoagulation. *Invest Ophthalmol Vis Sci.* 1994;35:4245–4252.
13. Pollack A, Heriot WJ, Henkind P. Cellular processes causing defects in Bruch's membrane following krypton laser photocoagulation. *Ophthalmology* 1986;93:1113–1119.
14. Del Priore LV, Glaser BM, Quigley HA, Green R. Response of pig retinal pigment epithelium to laser photocoagulation in organ culture. *Arch Ophthalmol.* 1989;107:119–122.
15. Wallow IH. Repair of the pigment epithelial barrier following photocoagulation. *Arch Ophthalmol.* 1984;102:126–135.
16. Young RW. Pathophysiology of age-related macular degeneration. *Surv Ophthalmol.* 1987;31:291–306.
17. Marmor MF. New hypotheses on the pathogenesis and treatment of serous retinal detachment. *Graefes Arch Clin Exp Ophthalmol.* 1988;226:548–552.
18. Weinberger D, Fink-Cohen S, Gaton DD, Priel E, Yassar Y. Non-retinovascular leakage in diabetic maculopathy. *Br J Ophthalmol.* 1995;79:728–731.
19. Roider J, Michaud NA, Flotte TJ, Birngruber R. Response of the retinal pigment epithelium to selective photocoagulation. *Arch Ophthalmol.* 1992;110:1786–1792.
20. Roider J, Hillenkamp F, Flotte TJ, Birngruber R. Microphotocoagulation: Selective effects of repetitive short laser pulses. *Proc Nat Acad Sci USA* 1993;90:8643–8647.
21. Roider J, Brinkmann R, Wirbelauer C, Laqua H, Birngruber R. Retinal sparing by selective retinal pigment epithelial photocoagulation. *Arch Ophthalmol.* 1999;117:1028–1034.
22. Roider J, Wirbelauer C, Brinkmann R, Laqua H, Birngruber R. Control and detection of subthreshold effects in the first clinical trial of macular diseases. *Invest Ophthalmol Vis Sci.* 1998;39 :104.
23. Roider J, Brinkmann R, Wirbelauer C, Laqua H, Birngruber R. Subtreshold (retinal pigment epithelium) photocoagulation in macular diseases: A pilot study. *Br J Ophthalmol.* 2000;84:40–47.
24. Framme C, Schuele G, Roider J, Birngruber R, Brinkmann R. Influence of pulse duration and pulse number in selective RPE laser treatment. *Laser Surg Med.* 2004;34:206–215.
25. Framme C, Brinkmann R, Birngruber R, Roider J. Autofluorescence imaging after selective RPE laser treatment in macular diseases and clinical outcome: A pilot study. *Br J Ophthalmol.* 2002;86(10):1099–1106.

26. Framme C, Roider J. Immediate and long-term changes of fundus autofluorescence in continuous wave laser lesions of the retina. *Ophthalmic Surg Lasers Imag*. 2004;35:131–138.
27. Kracht D, Brinkmann R. Green Q-switched microsecond laser pulses by overcoupled intracavity second harmonic generation. *Optics Commun*. 2004;231:319–324.
28. Holz FG, Bellmann C, Staudt S, Schutt F, Volcker HE. Fundus autofluorescence and development of geographic atrophy in age-related macular degeneration. *Invest Ophthalmol Vis Sci*. 2001;42:1051–1056.
29. Framme C, Kobuch K, Eckert E, Monzer J, Roider J. RPE in perfusion tissue culture and its response to laser application. Preliminary report. *Ophthalmologica* 2002;216:320–328.